

Butt-Coupling Loss of 0.1 dB/Interface in InP/InGaAs Multi-Quantum-Well Waveguide-Waveguide Structures grown by Selective Area Chemical Beam Epitaxy

C. A. VERSCHUREN, M. R. LEYS, H. VONK, J.H. WOLTER

Eindhoven University of Technology, Department of Physics

P.O.Box 513, 5600 MB Eindhoven, NL.

voice: +31 40 2474294; fax: +31 40 2461339; e-mail: j.wolter@phys.tue.nl

P. J. HARMSMA, Y. S. OEI

Delft University of Technology,

Department of Electrical Engineering, Delft, NL.

Received 01.03.1999

Abstract

The lateral coupling of waveguiding structures in both [011] and $[0\bar{1}1]$ directions is studied using embedded selective area epitaxy by Chemical Beam Epitaxy. All growth steps are carried out under the same growth conditions on (100) InP substrates misoriented by 0.5° towards (111)B. Both planar and selectively grown material exhibits bright luminescence and narrow PL line widths (8 meV FWHM at 4K), up to the lateral junction. Moreover, no degradation of the original material properties is observed after regrowth. SEM images show very flat layers and excellent lateral coupling for all four types of junctions. After reactive ion etching of waveguide ridges, the optical losses have been determined using a Fabry-Perot setup at 1530 nm (TE polarization). Values of 0.1 dB/interface with excellent uniformity are presented. From our results we conclude that by optimization of the sample preparation prior to regrowth, values of 0.1 dB/interface can be obtained reproducibly for both perpendicular coupling directions.

keywords: integrated optics, butt-coupling, SAE, CBE

Introduction

Monolithic integration of InP-based opto-electronic devices operating at $1.55 \mu\text{m}$ is increasingly important for applications such as WDM networks. For the best overall performance the different devices must be optimized individually and the coupling of the

optical signal from one device to another must be as efficient as possible. An attractive way for the production of such photonic integrated circuits (PICs) is embedded selective area epitaxy. By selective area growth in etched recesses, different vertically aligned structures with lateral (butt-)couplings can be realized, combining freedom in device design with an optimal overlap of the optical modes. In practice, the growth inside a recess is quite complex, especially near the side walls, where different crystallographic planes are exposed simultaneously and diffusion and shadowing effects influence the growth behaviour. This may lead to air gaps, local composition changes and severe growth rate changes, which can deteriorate the coupling efficiency.

In the last few years some groups have obtained promising results using low-pressure metalorganic vapor phase epitaxy (LP-MOVPE) [1] and chemical beam epitaxy (CBE) [2,3]. The latter CBE results are obtained by using a perpendicular group III injector instead of the usual tilted geometry. In this way shadowing effects are nearly eliminated, which is advantageous for the realization of good lateral couplings. Unfortunately, in most CBE systems, as in our Riber 32P, the perpendicular geometry is impossible. However, we find that the growth behaviour can be much improved by using a low substrate misorientation with only B type steps.

Here, we present our most recent results in InP/InGaAs multiple quantum well (MQW) waveguide-waveguide structures grown on substrates with a misorientation of $0.5^\circ \rightarrow (111)B$. We have achieved very good coupling results in both perpendicular crystallographic directions.

Experimental procedure

In the first epitaxy step MQW waveguide structures are grown by CBE in a Riber 32P system on 2 inch (100) InP substrates, 0.5° misoriented towards (111)B. The waveguiding core typically consists of 60 periods of 2 to 3 nm lattice matched InGaAs wells and 6 nm InP barriers, resulting in a room temperature photoluminescence at 1350-1400 nm. The top cladding layer of InP is 300 nm. Details of the growth can be found in [4]. After deposition of 100 nm SiN_x , series of windows are defined by lithography on quarter wafers. The mask pattern, illustrated in fig. 1, is aligned either in the $[011]$ or the $[0\bar{1}1]$ direction. It contains three groups of windows, each with five series of three identical windows, with lengths ranging from 100 to 900 μm , in steps of 200 μm . Using this mask recesses are etched by Reactive Ion Etching (RIE), through the WG core and about 200 nm into the InP buffer. The final step in sample preparation is a brief etch in diluted $\text{Br}_2/\text{CH}_3\text{OH}$. This gives a slight underetch below the SiN_x mask which, if properly applied, prevents the formation of so-called 'ears'. In the second growth step, the recesses are selectively filled with a similar WG structure using identical CBE growth conditions as for the original structure. Following the regrowth, 10 mm long waveguide stripes of 2, 3 and 4 μm width are defined in SiN_x , each running through one regrown recess, as indicated by the dashed lines in fig. 1. Near every series of regrown windows stripes are defined which only run through the original WG material, to serve as reference. The stripes are then used to etch shallow WG ridges, 100 nm into the core.

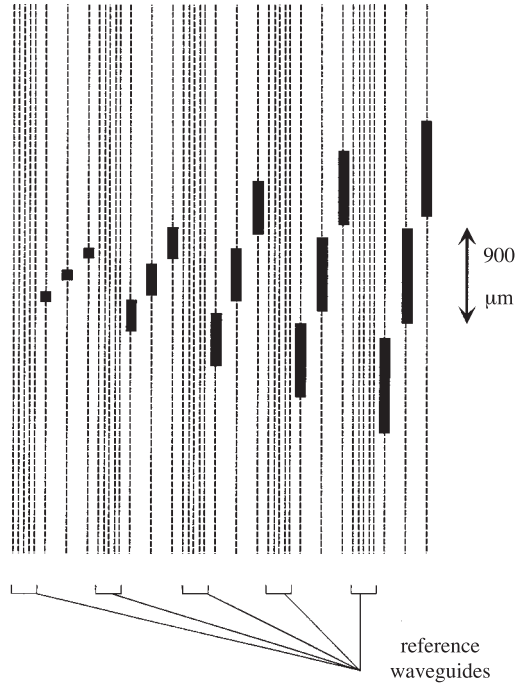


Figure 1. Schematic mask layout. The rectangles represent the windows/recesses for the selective regrowth, the dashed lines indicate the waveguide stripes for transmission measurements. This layout is repeated three times, with waveguide widths of 2, 3 and 4 μm , respectively.

Results and discussion

Waveguide substrates

Our 60 period MQW waveguide structures show bright luminescence and a high material quality, as indicated by e.g. the 4K PL linewidth of 7 to 9 meV and mirror-like morphology with low defect density. For the (original) waveguide substrates we use for the integration experiments, the PL peak positions at room temperature, λ_{RT} and the 4K linewidths are listed in table 1.

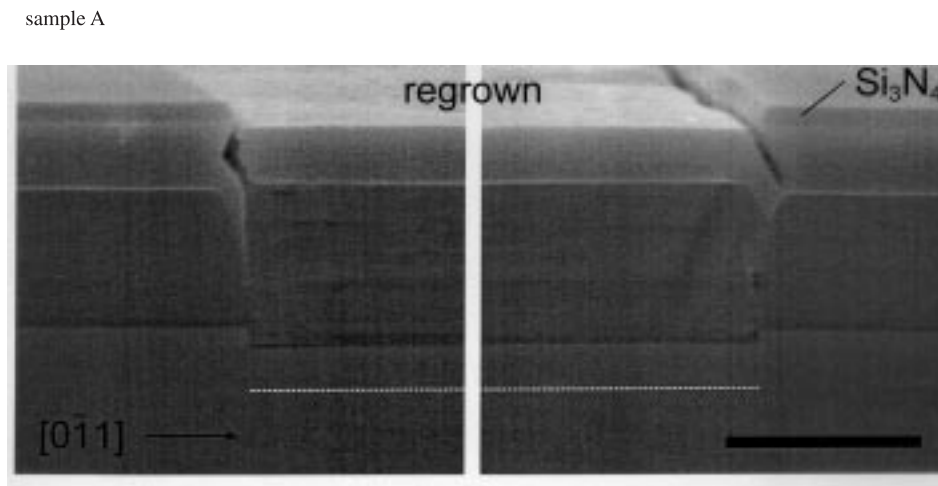
Table 1. Sample description

sample	lnP top (nm)	original λ_{RT} (nm)	WG 4K FWHM (meV)	regrown λ_{RT} (nm)	WG 4K FWHM (meV)	ridge direction	coupling loss (dB/interface)
A	300	1435	8	1400	9	[011]	0.3 ± 0.1
B	300	1415	9	1400	9	[011]	$< 0.1 \pm 0.04$

Integration results

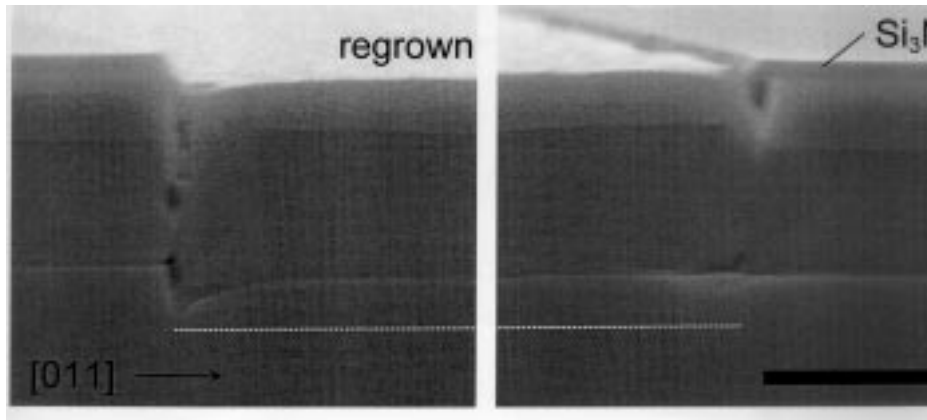
Characterization of both regrown material and coupling quality is important, since it provides information for the optimization of growth conditions and sample processing. The first method we use is Nomarski or phase contrast microscopy for a visual inspection of the surface. The morphology and the number of defects indicate mainly the success of the sample preparation and are a first check of the growth process. We find that the morphology in regrown areas is as smooth as on planar substrates, while the defect density is only slightly higher.

Information on the regrowth and coupling quality is obtained by examining cross sections using scanning electron microscopy (SEM). After cleavage, the samples are stain etched using $K_3Fe(CN)_6/KOH$ to enhance the material contrast. Fig. 2 shows the cross sections (see table 1 or sample details). It is clear that in all cases the vertical alignment and the flatness of the layers is excellent. The absence of air gaps and a transition over only about $0.1 \mu m$ suggest low coupling loss at the lateral interfaces. The coupling in figure 2.a (along $[0\bar{1}1]$) looks somewhat better than the coupling in fig. 2.b (along $[011]$). In our opinion this is because the combination of fast surface diffusion and chemically active B steps in the $[0\bar{1}1]$ direction helps to compensate shadowing effects at the recess side walls [5]. Notwithstanding the anisotropic diffusion, the results in fig. 2.b look surprisingly good.



(a)

sample B



(b)

Figure 2. SEM cross sections showing the lateral coupling for (a) sample A and (b) sample B. The dashed line shows the bottom of the etched recess, the bar indicates $1 \mu\text{m}$.

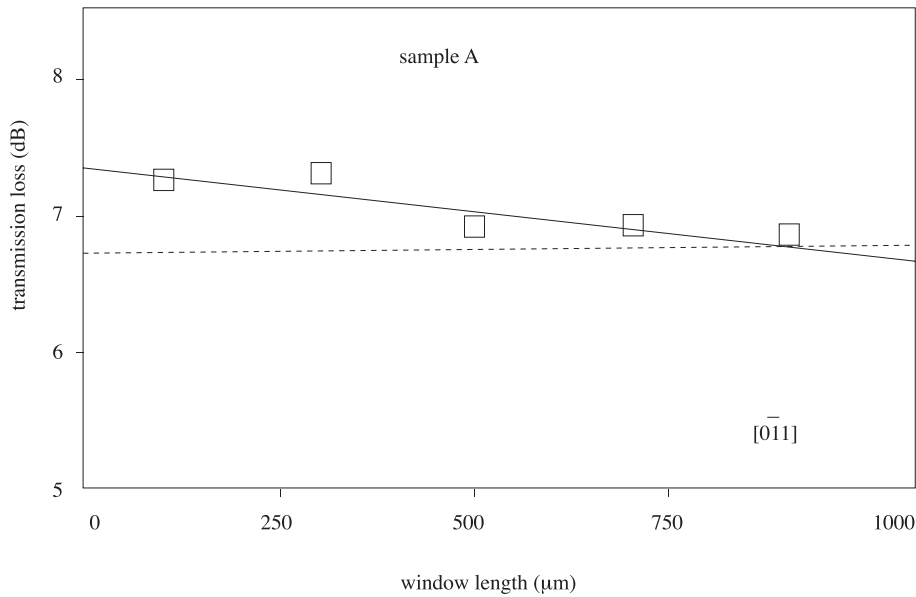
In order to check both original and regrown waveguide material properties after regrowth, we have used a spatially resolved PL (SRPL) setup with an Ar^+ laser focused to a spot diameter of about $5 \mu\text{m}$ and a He-flow cryostat which can be moved by two stepper motors with $0.1 \mu\text{m}$ step resolution. For the original WG we find no degradation or shift of the optical properties after regrowth. Both PL position and linewidth are the same within the experimental error of about 1 nm . The regrown material has PL intensities and linewidths which are uniform over the wafer and are comparable to that grown on 2 inch epi-ready substrates (see table 1).

The same SRPL setup is also used to quantify possible optical non-uniformities near the recess edges. With a scan along edges in the B type step propagation direction ($[0\bar{1}1]$), we find about 12 nm red shift, over a distance which extends more than $25\text{-}30 \mu\text{m}$ from the edge onto the regrown area. This distance corresponds to the surface corrugation that is always observed at this edge [5,6]. The red shift may be attributed to a locally enhanced growth rate at the macroscopic surface steps. The spectra for the three remaining edges, $[01\bar{1}]$, $[011]$ and $[0\bar{1}\bar{1}]$, are nearly identical. Analysis reveals a red shift of about 12 nm , but here it occurs within less than $1 \mu\text{m}$ from the edge. As indicated by high magnification SEM images, tiny (111) facets are formed near the recess side walls, which are known to give rise to a red shift [7,8]. We conclude that the actual extent of the red shift at these edges is about $0.1 \mu\text{m}$ or less.

We have determined the transmission loss for all waveguide ridges using a Fabry-Perot setup at 1530 nm (TE-polarization). Extrapolating the measured transmission losses to a regrown length of zero, and subtracting the reference's transmission loss, yields the loss due to the lateral interfaces only. The results for all samples are plotted in fig. 3.

The small scatter of the data around the curves illustrates the excellent uniformity of the lateral couplings. For sample A the transmission loss is reduced as the regrown length increases, which indicates that the regrown material has a loss smaller than that of the original material. This is caused by the different PL positions: the original material with $\lambda_{RT}=1430$ nm gives rise to significant absorption at 1530 nm, while the regrown material with $\lambda_{RT}=1390$ nm is more transparent. It is clear that for negligible absorption effects, λ_{RT} must be well below 1400 nm.

From the data in fig. 3.a we obtain a coupling loss for sample A of about 0.6 dB for 2 lateral interfaces ($=2\epsilon_i$) along $[0\bar{1}1]$. Since no irregularities are observed in the SEM cross sections (fig. 2.a) part of this loss is attributed to the observed corrugation related red shift over a distance of more than 25 μm . Thus, it should be possible to reduce this coupling loss by growing material with a lower λ_{RT} . Fig. 3.b shows equal values for both reference and partly regrown waveguides. Since no dependence on the regrown length is observed, the coupling loss is in fact determined by the standard deviation of the measurements, resulting in a *maximum* values as low as $\epsilon_i=0.1\pm 0.04$ dB/interface for sample B. These results are clearly not optimal. However, further experiments [4] indicate that coupling losses around 0.1 dB/interface can be reproducibly achieved in both crystallographic directions.



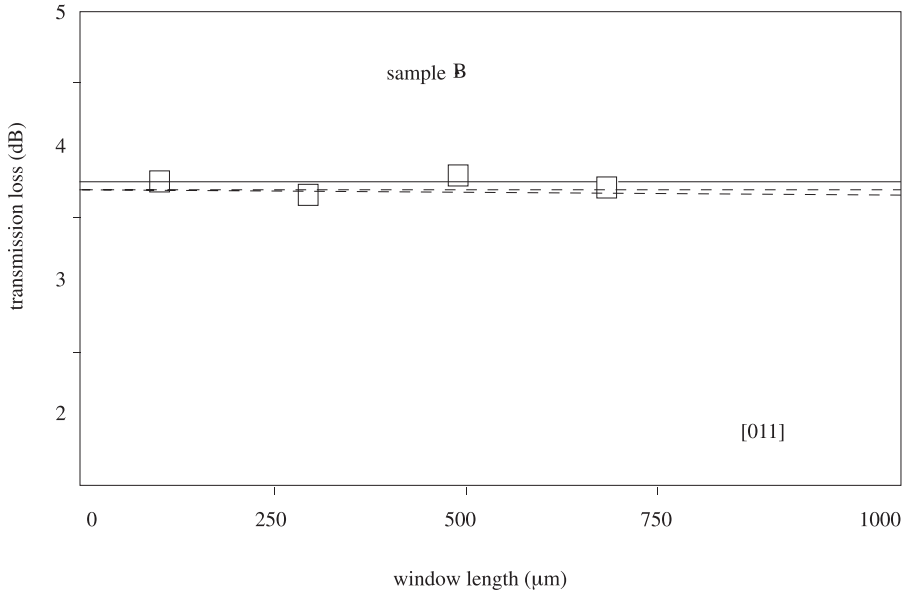


Figure 3. Fabry-Perot transmission measurements versus the length of a regrown window for $3 \mu\text{m}$ WG ridges. The dashed lines represent the reference waveguide data.

Conclusions

We have investigated the lateral integration of waveguiding structures by embedded selective area Chemical Beam Epitaxy using $(100) \text{InP } 0.5^\circ \rightarrow (111)\text{B}$ substrates. The second growth step is carried out under identical growth conditions as the first, planar growth step. PL characterization shows no degradation or shift for the original material after regrowth. Furthermore, the morphological and PL quality of the regrown material is as good as on normal substrates, up to the lateral junction. SEM and Fabry-Perot measurements reveal very good coupling results with excellent uniformity in both perpendicular crystallographic directions. At the $[0\bar{1}1]$ junction a small PL red shift is observed for the regrown structures. To eliminate resulting absorption effects in regrown passive structures, λ_{RT} must be below $\sim 1380 \text{ nm}$. For planar regrowth surfaces, growth irregularities or ‘ears’ at the recess edge must be prevented. This can be done by carefully underetching the reactive ion etched recess prior to the regrowth. Loss values around 0.1 dB/interface can be realized for lateral coupling along both $[011]$ and $[0\bar{1}1]$, which is extremely attractive for applications in the integration of photonic devices.

Acknowledgements

This work was financially supported by the Dutch Ministry of Economic Affairs (IOP) and the ACTS programme of the European Union. Special thanks to Geraldine O’Donovan for carrying out the spatially resolved photoluminescence measurements.

References

- [1] J. H. Ahn, K. R. Oh, J. S. Kim, S. W. Lee, H. M. Kim, K. E. Pyun and H. M. Park, IEEE Photon. Technol. Lett. 8 (1996) 200.
- [2] P. Legay, F. Alexandre, J. L. Benchimol, M. Allovon, F. Laune and S. Fouchet, J. Crystal Growth 164 (1996) 314.
- [3] M. Wachter, U. Schöffel, M. Schier and H. Heinecke, J. Crystal Growth 175/176 (1997) 1186.
- [4] C. A. Verschuren, P. J. Harmsma, Y. S. Oei, M. R. Leys, H. Vonk and J. H. Wolter, J. Crystal Growth, 188 (1998) 288.
- [5] C. A. Verschuren, M. R. Leys, Y. S. Oei, C. G. M. Vreeburg, H. Vonk, R. T. H. Rongen and J. H. Wolter, J. Crystal Growth 170 (1997) 650.
- [6] R. Matz, H. Heinecke, B. Baur, R. Primig and C. Cremer, J. Crystal Growth 127 (1993) 230.
- [7] H. Heinecke, A. Milde, R. Matz, B. Baur and R. Primig, Physica Scripta Vol T55 (1994) 14.
- [8] T. H. Chiu, Y. Chen, J. E. Zucker, J. L. Marshall and S. Shunk, J. Crystal Growth 127 (1993) 169.